Global Journal of Engineering and Technology Advances
eISSN: 2582-5003
Cross Ref DOI: 10.30574/gjeta
Journal homepage: https://gjeta.com/

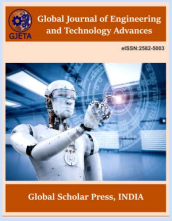

(Research Article)

Check for updates

Comparison of analytical and numerical simulations of cowpea (*Vigna unguiculata*) grain drying using Fick's law and the finite element method

Marco Aurélio Amarante Ribeiro *

Doctoral Student, Federal University of Viçosa (UFV), Viçosa, MG, Brazil.

Global Journal of Engineering and Technology Advances, 2025, 23(02), 001-015

Publication history: Received on 17 March 2025; revised on 27 April 2025; accepted on 30 April 2025

Article DOI: https://doi.org/10.30574/gjeta.2025.23.2.0139

Abstract

This article presents a comprehensive analysis of the drying process of a single cowpea bean (Vigna unguiculata) using both analytical and numerical approaches. The process, governed by coupled heat and mass transfer (Bird et al., 2002) mechanisms, was simulated by modeling the bean as an ellipsoidal body under isotropic conditions. The analytical solution was based on a truncated series representation of Fick's second law, while the numerical solution employed the Finite Element Method (FEM) with convective boundary conditions. Simulations were implemented in Python, incorporating thermophysical properties of air and grain derived from empirical models in the literature. Drying behavior at different temperatures was evaluated, and the results from both methods were compared using relative error and standard error of the estimates. The two solutions exhibited strong agreement, particularly during the active drying phase, confirming the accuracy and robustness of both modeling strategies. This comparative study contributes to the development of accurate thin-layer drying models (Madamba, 1996) and supports the optimization of post-harvest processing techniques.

Keywords: Drying Process Modeling; Finite Element Method; Fick's Second Law; Moisture Diffusion; Cowpea

1. Introduction

Cowpea (*Vigna unguiculata* (L.) Walp.), commonly known in Brazil as feijão-de-corda, feijão-macassar, or feijão-fradinho, is a legume of significant socioeconomic importance, particularly in the North and Northeast regions of the country. Adapted to semi-arid climates and low-fertility soils, cowpea is notable for its resilience, short growth cycle, and high drought tolerance. These characteristics make it a strategic crop for food security in areas with challenging edaphoclimatic conditions. In addition to serving as a vital source of plant-based protein in local diets, cowpea cultivation sustains the livelihoods of smallholder farmers and is widely used for both fresh consumption and industrial processing, such as flour production and traditional regional dishes. Brazil ranks among the world's leading cowpea producers, with significant advancements in breeding programs aimed at increasing productivity, resistance to pests and diseases, and the nutritional quality of the grains (Freire Filho et al., 2012).

Grain drying, regardless of type, is a critical stage in post-harvest crop handling, as it directly impacts the shelf life, quality, and usability of the final product. A solid understanding of the fundamental principles underlying the drying process is essential for optimizing drying technologies and improving operational efficiency. At its core, grain drying involves the transfer of heat and water from the grain to the surrounding air, governed by a series of physical and thermodynamic mechanisms (Chen & Pan, 2023). These principles have been extensively documented in the literature (Brooker et al., 1974; Pabis et al., 1991; Brooker et al., 1992; Bengtsson & Ahrné, 2005; Jian & Jayas, 2022).

* Corresponding author: Marco Aurélio Amarante Ribeiro

During the initial drying phase, surface water evaporates rapidly, maintaining a constant drying rate. This stage is primarily influenced by the availability of heat and the efficiency of mass transfer between the grain and the drying medium, typically air (Bird et al., 2002; Li et al., 2023). As drying progresses, the process transitions into a falling-rate period, during which water migrates from the interior to the surface. The drying rate gradually declines due to reduced water gradients and increasing internal resistance to water movement (Jayas et al., 2023). Eventually, the grain reaches its equilibrium water content, at which point further drying becomes negligible.

The drying process encompasses both heat and mass transfer phenomena. Heat may be delivered by conduction, convection, or radiation, depending on the drying technique employed. This thermal energy increases the grain's temperature, facilitating internal water movement toward the surface. However, excessive or uneven heating can degrade grain quality, leading to structural damage or uneven drying (Jibril et al., 2024). Mass transfer, defined as the movement of water from within the grain to the surface for evaporation, is influenced by factors such as grain temperature, relative humidity, and airflow conditions (Zhang et al., 2006).

Several mathematical models have been developed to describe drying kinetics and predict the rate of water removal. Thin-layer drying models—such as the Page (Page, 1949), Midilli, and Henderson and Pabis (Henderson & Pabis, 1961) models—are widely applied to represent the drying behavior of grains, including cowpea (Jayas et al., 2023). These models typically assume a single-layer configuration and express the drying process in terms of water content ratio and time. A key parameter in these models is the effective water diffusivity, which quantifies the ease of internal water migration and is influenced by temperature, initial water content, and the physical properties of the grain (Li et al., 2023).

Energy consumption is another important consideration, as drying is one of the most energy-intensive stages in post-harvest processing. Assessing the energy balance during drying is fundamental to developing sustainable and energy-efficient technologies (Jimoh et al., 2023; Jibril et al., 2024).

Environmental conditions also play a significant role in drying performance. High air temperatures typically accelerate drying but may compromise product integrity if not carefully controlled. Similarly, high ambient humidity levels can reduce the moisture gradient between the grain and the air, slowing the process (Chen & Pan, 2023). Airflow velocity is also crucial, as sufficient air circulation promotes uniform moisture removal (Sahin & Sumnu, 2006).

Various drying technologies have been developed, each with specific advantages and limitations. Hot air drying is the most commonly used method, valued for its simplicity and cost-effectiveness, although it may result in uneven drying if not properly controlled (Jayas et al., 2023). More advanced systems, such as fluidized bed dryers, promote uniformity through constant grain agitation, while freeze and vacuum drying offer superior preservation of nutritional content at higher energy costs (Ho, 1992).

Given the complexity of drying—which involves coupled heat and mass transfer mechanisms—advanced simulation tools are essential. Modeling the drying of a single grain allows for precise analysis of internal water diffusion and surface interactions. Both analytical and numerical methods have been employed for this purpose. Analytical solutions, based on Fick's law, provide valuable theoretical insight, while numerical approaches such as the Finite Element Method (FEM) offer greater versatility and accuracy for grains with complex geometries.

This work aims to compare these two modeling approaches—analytical and numerical (FEM)—in simulating the drying of a single cowpea grain. The grain is modeled as an ellipsoid with isotropic properties. The simulation incorporates convective boundary conditions and uses thermophysical data derived from empirical models and published literature. FEM implementation was carried out using Python-based algorithms to solve the diffusion equation under realistic drying scenarios, with the goal of evaluating the strengths and limitations of each modeling strategy.

2. Fundamental Considerations

Single grain drying can be described as a water removal process in which water is transferred from the grain surface to the atmosphere, usually through evaporation. This process is influenced by several factors, such as air temperature, air velocity, relative humidity, and physical properties of the grain. Characteristics such as porosity, shape, size, and thermal conductivity play a crucial role in the drying rate, and these factors can vary significantly according to the grain type, which makes modeling single grain drying a considerable technical challenge (Dincer & Dost, 2019; Iqbal et al., 2020).

Grain drying modeling has been an important field of study due to its relevance in several industrial processes, such as agriculture and food production. Modeling the grain drying process fundamentally depends on the analysis of heat and

mass transfer (Albini, Freire, & Freire, 2019; Bird et al., 2002) phenomena in a thin layer of grains and their interactions with the drying medium. Understanding these phenomena is obtained through the analysis of a single grain, since a thin layer of grains is usually formed by a mesh with the thickness of a single grain, uniformly arranged on a tray with a perforated bottom. Thus, modeling a single grain allows greater precision in modeling the drying of thin layers of grains.

Numerous researchers have effectively employed the Finite Element Method (FEM) to simulate the drying behavior of individual grains (Haghighi et al., 1990; Irudayaraj, 1993; Jia et al., 2002). The drying of a single grain involves complex challenges arising from its geometry, thermophysical properties, and the dynamic nature of moisture transport within the material. To better understand and optimize this process, mathematical modeling and numerical simulations are essential tools. Among the available approaches, this study focuses on comparing the analytical solution of the diffusion equation with the numerical solution provided by FEM, considering the bean grain as an ellipsoidal body.

3. Methodology

This study focused on modeling the drying process of a single cowpea bean grain, idealized as an ellipsoidal body with isotropic properties, through a comparative analysis of two simulation approaches: the analytical solution of Fick's second law of diffusion (Goneli et al., 2010) and the Finite Element Method (FEM). This comparative modeling is essential for understanding thin-layer drying phenomena and extends to applications in thick-layer drying systems, offering insights that contribute to process optimization and equipment design (Crank, 1975; Dincer & Dost, 2019; Kudra & Mujumdar, 2002).

The modeling was performed by integrating the numerical solution of the diffusion equation using FEM under convective (Robin-type) boundary conditions, and comparing the results with those obtained via the classical analytical series solution. The numerical approach was implemented in Python (Hunter, 2007; Harris et al., 2020; Virtanen et al., 2020), and it relied on empirical models and thermophysical correlations to define the physical properties of the grain and air under drying conditions, supplemented by data from established literature sources (Jamaleddine & Ray, 2010; Iqbal, Haider, & Sattar, 2020; Liu, Zhang, & Wang, 2017).

The FEM framework enabled the solution of the diffusion equation in a three-dimensional domain, making it particularly appropriate for grains with non-spherical geometries. Within this framework, the governing partial differential equations were discretized through the assembly of mass matrices, stiffness matrices (representing the diffusion term), and boundary matrices (modeling the convective flux), in line with standard finite element procedures (Bird, Stewart, & Lightfoot, 2002; COMSOL, 2017). This methodology offers flexibility in the definition of material properties, meshing strategies, and boundary conditions—features often limited in purely analytical approaches (Ramachandran et al., 2018; Arsène, Hénault, & Lefebvre, 2021).

Additionally, the weak form of Fick's second law used in FEM enables precise temporal and spatial resolution, especially when implicit time discretization schemes are employed. The implementation conducted in this study utilized Python-based algorithms, which are particularly effective for the numerical simulation of mass transfer processes in complex geometries (Fish & Belytschko, 2007).

3.1. Classic Drying Models

It is necessary to report on empirical drying models because they are frequently used to represent grain drying, especially for modeling grain drying in thin layers with a thickness of one grain, to obtain the drying curve under isothermal conditions under controlled conditions. These equations are fundamental for applications in modeling thick layer drying on a commercial scale.

These empirical models are built from adjustments to experimental data, when there is little experimental data or the complexity of the system does not justify the use of advanced numerical methods, generally with simple expressions and few parameters, while semi-empirical models try to incorporate a simplified physical basis, incorporating better adjustment capacity, although they continue to maintain a degree of empiricism.

Some simpler classical models are presented below, although a variety of these models are found in the literature, but in some ways, they are all modifications of these classical models.

3.1.1. Lewis model

This model is the simplest one used to describe the drying rate according to the difference between the grain moisture content and the equilibrium moisture content, derived directly from the analytical solution of the first-order Fick's law,

assuming one-dimensional and isothermal diffusion. This model is effective when drying occurs uniformly, usually in the constant-rate period, typical of products with high initial moisture content, as expressed by Equation (1):

$$M_R = \frac{M(t) - M_e}{M_0 - M_e} = e^{-k \cdot t} \ldots\ldots\ldots\ldots\ldots (1)$$

where

M_R – Water content ratio.

$M(t)$ – Grain water content over time, [kg water/kg dry air].

M_0 – Initial water content of the grain, [kg water/kg dry air].

M_e – Equilibrium water content, [kg water/kg dry air].

t – Time, [s]

k – Drying rate constant, [s^{-1}]

3.1.2. Page model

Another widely used model is known as the Page Model, due to its simplicity and ability to describe drying at various stages of the process, such as flash drying, using an exponential function (Page, 1949):

$$M_R = exp(-k \cdot t^n) \ldots\ldots\ldots\ldots\ldots\ldots (2)$$

where n is an exponent that depends on the drying conditions.

3.1.3. Henderson and Pabis model

This model is a simplified version of the Lewis model, but with a multiplicative coefficient that improves the fit, assuming an exponential loss of water from the grain over time, without taking into account the complexity of non-linear variations in the drying rate (Henderson & Pabis, 1961):

$$M_R = a \cdot exp(-k \cdot t) \ldots\ldots\ldots\ldots\ldots (3)$$

where a is an adjustment coefficient that depends on the drying conditions.

These models are widely used due to their simplicity and excellent performance in nonlinear regression with experimental data, although they disregard the effects of internal gradients, resistances and variations in physical properties.

3.2. Models based on the Three-Dimensional Diffusion Equation

The drying process of a single grain involves heat transfer due to the hot air surrounding it and also the migration of water from the interior to the surface of the grain, where evaporation occurs. Therefore, it involves a process of simultaneous heat and mass transfer (Bird et al., 2002) described by the equations of conservation of mass and conservation of energy. The fundamental equations for simulating the drying of a grain are presented below.

3.2.1. Physical Basis of the Diffusion Model

The internal diffusion of water in capillary-porous media can be described by Fick's Second Law in three dimensions, which is a partial differential equation (PDE) that models the propagation of water in a diffusive medium:

$$\frac{\partial u}{\partial t} = D_{ef} \cdot \left(\frac{\partial^2 u}{\partial x^2} + \frac{\partial^2 u}{\partial y^2} + \frac{\partial^2 u}{\partial z^2} \right) \ldots\ldots\ldots\ldots\ldots (4)$$

or in vector form

$$\frac{\partial u}{\partial t} = D_{ef} \cdot \nabla^2 u \; ; \quad u = u(x, y, z, t) \ldots\ldots\ldots\ldots\ldots (5)$$

were

- u – Water concentration (or water content, dry basis), [kg/m^3].
- t – Time, independent variable that represents the temporal evolution of drying, [s]
- D_{ef} – Effective diffusion coefficient, [m^2/s]
- $\frac{\partial u}{\partial t}$ – Partial derivative of u with respect to t, representing the temporal variation of water content, [kg water/(kg dry air) · s].
- $\nabla^2 u$ – Laplacian operator, which represents the sum of the second derivatives in each spatial direction.

Equation (4) is used to describe the migration of water from the interior of the grain to its surface. For grains with regular geometry—such as spheres or ellipsoids—it can be solved analytically using an infinite Fourier series, and numerically for any geometry using the Finite Element Method-FEM (Fish & Belytschko, 2007) or Finite Volume Method-FVM.

3.2.2. Initial conditions

$$u(x, y, z, 0) = u_0(x, y, z) \ldots\ldots\ldots\ldots\ldots (5)$$

It indicates that at the initial instant $t = 0$, the distribution of water content u inside the grain is known and given by a function u_0.

3.2.3. Dirichlet boundary conditions

It considers the fixed water content at the surface and defines the imposed surface water content, $u_s|_\Gamma$, directly at the boundary Γ:

$$u|_\Gamma = u_s(t) \ldots\ldots\ldots\ldots\ldots (7)$$

3.2.4. Neumann boundary conditions

Maintains fixed flow (impermeable surface), indicating that there is no water flow in the normal direction n to the outer surface:

$$\left.\frac{\partial u}{\partial n}\right|_\Gamma = 0 \ldots\ldots\ldots\ldots\ldots\ldots (8)$$

3.2.5. Robin type boundary condition

Defines the mass exchange by convection between the grain and the external air, where h_m is the mass transfer coefficient (Incropera et al., 2007) and u_e is the equilibrium water content of the grain in contact with the air (dry basis). Diffusivity is also used in the convective boundary condition in the numerical solution of the diffusion equation by the finite element method, expressed by Equation (9):

$$-D_{ef}\frac{\partial u}{\partial n} = h_m(u - u_e) \ldots\ldots\ldots\ldots\ldots (9)$$

Here comes the mass transfer coefficient (Incropera et al., 2007), h_m, which can be estimated with correlations of the Sherwood number type, as a function of the Reynolds and Schmidt numbers:

$$Sh = 0{,}2 + 0{,}6 \cdot Re^{1/2} \cdot Sc^{1/3} \ldots\ldots\ldots\ldots (10)$$

3.2.6. Reynolds number

$$Re = \frac{\rho_a \cdot v \cdot d_{eq}}{\mu} \ldots\ldots\ldots\ldots\ldots (11)$$

3.2.7. Schmidt number

$$Sc = \frac{\rho_a}{\rho_a \cdot D_a} \dots\dots\dots\dots\dots (12)$$

3.2.8. Sherwood number

$$Sh = \frac{h_m \cdot d_{eq}}{D_a} \dots\dots\dots\dots\dots\dots (13)$$

3.2.9. Analytical Solution of the Diffusion Model

For an ellipsoidal grain with equivalent radius, r_{eq}, assuming symmetry and constant diffusivity, the water content ratio can be expressed by a series of sines and exponentials:

$$M_R(t) = \sum_{n=1}^{\infty} \left(\frac{6}{n^2 \cdot \pi^2}\right) \cdot exp\left[(-n^2 \cdot \pi^2)\left(\frac{D_{ef} \cdot t}{r_{eq}^2}\right)\right] \dots\dots\dots\dots (14)$$

where the equivalent radius of the ellipsoid with axes a, b, c is given by:

$$r_{eq} = \sqrt[3]{a \cdot b \cdot c} \dots\dots\dots\dots\dots (15)$$

This analytical expression considers the Fick solution with uniform Dirichlet boundary condition on the surface. Therefore, the greater the number of terms in the series, the greater the accuracy.

The thermal dependence of diffusivity can be expressed by the Arrhenius equation (Dincer & Dost, 2019):

$$D_{ef}(T) = D_0 \cdot exp\left(-\frac{E_a}{R \cdot T}\right) \dots\dots\dots\dots\dots (16)$$

The sensitivity of diffusivity to temperature varies non-linearly according to the variation of the activation energy, E_a.

3.3. Numerical Formulation by the Finite Element Method

The Finite Element (FEM) formulation solves the weak equation of Fick's Second Law, with a Robin (convective) boundary condition. This formulation allows solving the diffusion equation considering complex geometries, heterogeneities in the medium and varied boundary conditions. The weak formulation of the Fick equation with a Robin (convective) boundary condition:

$$\int_{\Omega} v \frac{\partial u}{\partial t} d\Omega + \int_{\Omega} D_{ef} \nabla u \cdot \nabla v \, d\Omega = \int_{\Gamma} h_m (u - u_e) \, v \, d\Gamma \dots\dots\dots\dots (17)$$

The discretized equations for implementation in finite elements are presented below.

3.3.1. Mass matrix

The mass matrix ($\boldsymbol{M}$) is a fundamental component in the solution of transient models by the finite element method:

$$\boldsymbol{M_{ij}} = \int_{\Omega} \phi_i \phi_j \, d\Omega \dots\dots\dots\dots (18)$$

Where;

$\boldsymbol{M_{ij}}$ – Term representing the water content coupling between nodes i and j.

Ω – Body domain (bean grain).

ϕ_i, ϕ_j – Shape functions associated with element nodes.

The mass matrix represents the inertia of the drying system in accumulating or releasing water (water vapor) and, by analogy with heat transfer, is equivalent to thermal capacitance. This matrix reflects the distribution of water contained in the grain and its evolution over time.

3.3.2. Stiffness matrix (diffusion)

The stiffness matrix (***K***) represents the internal flux of water (vapor), caused by spatial differences in concentration, and models the coupling of the domain with the external environment through surface convection. This matrix represents the resistance or ease with which the material loses water to the external environment, acting analogously to a surface conductance in heat transfer. This matrix represents the diffusion of water within the grain domain and originates from the term containing the water content gradient in the weak formulation:

$$\boldsymbol{K_{ij}} = \int_{\Omega} D_{ef} \nabla \phi_i \cdot \nabla \phi_j \, d\Omega \; \ldots\ldots\ldots\ldots\ldots (19)$$

Where;

$\mathbf{K_{ij}}$ – It represents the diffusion of water within the grain domain.

D_{ef} – Effective diffusion coefficient.

$\nabla \phi_i$ – Gradient of the shape function associated with the node. i

The matrix ***K*** is only assembled on the boundary elements (elements with faces on the grain surface), is additive to the global system and appears together with the stiffness matrix in the time advance equation.

3.3.3. Contour matrix (Robin condition)

The boundary matrix appears in the finite element formulation when a Robin-type boundary condition is used, generating an additional term in the weak formulation of the Fick's equation and contributing an additional matrix called the boundary matrix ***R***:

$$\boldsymbol{R_{ij}} = \int_{\Gamma} h_m \phi_i \phi_j \, d\Gamma \; \ldots\ldots\ldots\ldots\ldots (20)$$

Where

Γ	–	Outer boundary of the domain (grain surface).
ϕ_i, ϕ_j	–	Shape functions associated with surface nodes.
h_m	–	Mass transfer coefficient (m/s).
$\boldsymbol{R_{ij}}$	–	Stiffness term - resistance to water diffusion or heat conduction.

3.3.4. Source font vector

The surface source vector (***F***) represents the effect of mass exchanges between the grain surface and the environment (air), derived from the Robin (or convection) boundary condition:

$$\boldsymbol{F_i} = \int_{\Gamma} h_m u_e \, \phi_i \, d\Gamma \; \ldots\ldots\ldots\ldots\ldots (21)$$

Where

$\boldsymbol{F_i}$ – Surface source vector of element i.

u_e – Equilibrium water content at the surface.

ϕ_i – Shape function associated with node i on the surface.

This vector is responsible for quantifying the gain or loss of water (water vapor) across the grain boundary.

3.3.5. Matrix system after implicit temporal discretization

After discretizing Equation (17), the matrix system represented in Equation (22) appears:

$$[\boldsymbol{M} + \Delta t(\boldsymbol{K} + \boldsymbol{R})] \cdot \boldsymbol{u}^{n+1} = M \cdot \boldsymbol{u}^{n} + \Delta t \cdot \boldsymbol{F} \ldots\ldots\ldots\ldots\ldots (\mathbf{22})$$

Where;

$\boldsymbol{M}$ – Mass matrix.

$\boldsymbol{K}$ – Stiffness matrix (diffusivity).

$\boldsymbol{R}$ – Boundary matrix (convection).

$\boldsymbol{u}^{n}$ – Water content vector in time t_n.

3.3.6. Comparison of the Efficiency of Analytical Solution and Finite Element Solution

A comparison of the efficiency of the analytical series solution of the diffusion equation (with a large number of terms), in relation to the finite element solution, is found in Table 1.

Table 1 Comparison between Analytical and Finite Element Solutions.

Feature	**Analytical Solution**	**Finite Element Solution**
Geometry	Requires ideal symmetry	Any geometry
Boundary condition	Dirichlet (usually)	Dirichlet, Neumann or Robin
Precision	High (with many terms)	High (depending on mesh and method)
Flexibility	Limited	High
Computational cost	Low	Moderate to high

3.4. Method for Comparing Results

The results of the simulations using the two solution methods were compared using two statistical parameters:

Relative Error

$$E_r = \left| \frac{M_R^{FEM}(t) - M_R^{Anal}(t)}{M_R^{Anal}(t)} \right| \cdot 100 \ldots\ldots\ldots\ldots\ldots (23)$$

Where

E_R – Relative error, [%]

M_R^{FEM} – Water content ratio value simulated using finite elements.

M_R^{Anal} – Water content ratio value simulated using analytical solution of diffusion equation with thirty terms.

3.4.1. Standard Error of Estimates

$$S_{EE} = \sqrt{\frac{1}{n}\sum_{i-1}^{n}(y_i - \hat{y}_i)^2} \ldots\ldots\ldots (24)$$

Where

S_{EE} – Standard deviation between predicted and observed values.

y_i – Observed or experimental value.

$\hat{y}_i$ – Value estimated or predicted by the model.

n – Number of observations.

3.5. Diffusion Model Solution

Two solutions were presented: (i) analytical solution using 30 terms of the Fick series, Equation (14), and (ii) numerical solution implemented in a Python algorithm, using the finite element method, considering a bean as an isotropic ellipsoid (Figure 1).

The mathematical formulation was implemented in an algorithm coded in Python language to perform the simulations, prepare the data tables and graphs of the drying curves. For the numerical solution, the ellipsoidal geometry of a cowpea grain, as illustrated in Figure 1, with axes a = 9 mm, b = 6 mm, c = 5 mm, was discretized into a mesh 20 × 20 × 20, resulting in approximately 10,000 elements. An illustration of the discretization mesh is shown in cross-section in Figure 2. The drying conditions established for the simulations, with a drying air flow with a speed equal to 1 m/s are in Table 2 and the physical properties of the bean grain (Goneli et al., 2010) are in Table 3.

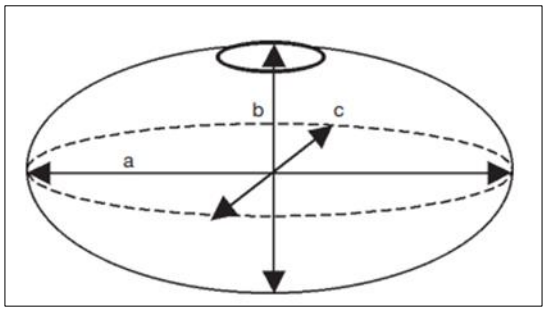

(A)

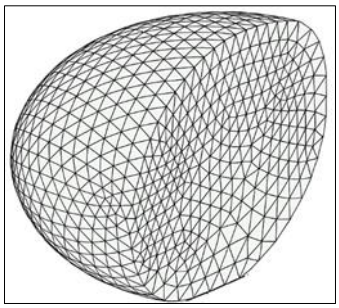
(B)

Figure 1 (a) Ellipsoidal geometry assumed for a cowpea grain, and (b) Illustration of the finite element mesh


(A)

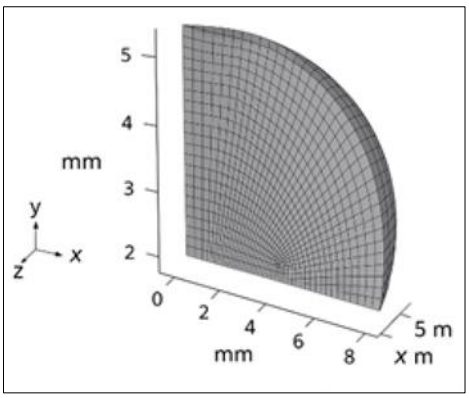

(B)

Figure 2 (a) Illustrative image of a cowpea grain, and (b) mesh with, approximately, 10,000 elements of a quarter of the ellipsoid representing the cowpea grain

3.5.1. Physical properties of dry air

Table 2 Physical properties of dry air as a function of temperature in the range from **0**°C ***to*** **100**°C.

Property	**Unit**	**Equation**
Density:	kg/m^3	$\rho_a(T) = \frac{101325}{287{,}05 \cdot (T + 273{,}15)}$
Dynamic viscosity:	$Pa \cdot s$	$\mu(T) = \mu_0 \cdot \left(\frac{T_0 + C}{T + C}\right) \cdot \left(\frac{T}{T_0}\right)^{3/2}$

		$\mu_0 = 1{,}716 \times 10^{-5}\ Pa \cdot s$ $T_0 = 273{,}15\ K$ $C = 111$
Specific heat:	J/kg · K	$c_a = 978{,}685 + 0{,}1 \cdot T$
Thermal conductivity:	W/m · K	$k(T) = 0{,}0244 + 0.000075 \cdot (T - 273{,}15)$
Mass diffusivity of water vapor in air:	m^2/s	$D_a(T) = 2{,}06 \times 10^{-5} \cdot \left(\frac{T}{273{,}15}\right)^{1{,}81}$
Thermal diffusivity:	m^2/s	$\alpha_a = \frac{k}{\rho_a \cdot c_a}$

3.5.2. Physical properties of beans

Table 3 Physical properties of beans as a function of water content and temperature**.**

Property	**Unit**	**Equation**
Bulk Density:	(kg/m^3)	$\rho_{gb} = 853{,}3 - 4{,}5 \cdot M$
Actual density:	(kg/m^3)	$\rho_{gr} = 1220 + 1{,}8 \cdot M$
Porosity:	(%)	$\varepsilon = \left(1 - \frac{\rho_{gb}}{\rho_{gr}}\right) \cdot 100$
Specific heat:	(kJ/kg · K)	$c_g = 1{,}38 + 0{,}025 \cdot M$
Effective diffusion coefficient:	(m^2/s)	$D_{ef}(T) = D_0 \cdot exp\left(-\frac{E_a}{R \cdot T}\right)$
Pre-exponential factor:	(m^2/s)	$D_0 = 1{,}701 \times 10^{-3}$
Activation energy:	(J/mol)	$E_a = 42843$
Thermal conductivity:	(W/m · K)	$k = 0{,}18 + 0.003 \cdot M$
Thermal diffusivity:	(m^2/s)	$\alpha_g = \frac{k}{\rho_{gr} \cdot c_g}$

4. Results and discussion

The simulation results were obtained using a computational program written in Python to simulate the drying of a cowpea grain (Vigna unguiculata (L.) Walp.) using 30 terms from the series solution of Fick's law and a element mesh inside an ellipsoid with axes of dimensions, and for the numerical solution. For the analytical solution, spherical coordinates were used with an equivalent radius of, based on the dimensions of the ellipsoidal axes representing the bean grain (Goneli et al., 2010).

The physical properties of air and grain used in the simulations were obtained using the equations presented in Tables 2 and 3, for drying conditions with an air flow velocity of 1 m/s, temperatures of 40°C, 60°C, and 70°C, initial grain water content equal to 30 % $b.u.$ (0,429 $b.s.$) , as initial conditions, equilibrium grain water content equal to 4,8 % $b.u.$ (0,05 $b.s$), as boundary conditions for the analytical solution, and initial grain temperature equal to 25°C. For the finite element solution, the Robin convective boundary condition was used. The results are presented in Tables 4 and in the graph in Figure 2.

Table 2 shows that the moisture ratio of the grain did not reach equilibrium ($MR = 0$) after 20 hours of drying at 40 °C, indicating that a little more time is needed to reach equilibrium. This is due to the slower drying rate at lower temperatures, which requires more time to achieve equilibrium under the drying conditions imposed by an air flow velocity of 1 m/s.

At a temperature of 60 °C, the grain's moisture ratio practically reaches its equilibrium value after 16 hours ($MR \approx 0$). Beyond this point, the results become irrelevant, as any further mass loss indicates loss of dry matter rather than water (the data block is highlighted in yellow).

Similarly, at 70 °C, the grain's moisture ratio reaches equilibrium around 11 hours of drying. Therefore, results beyond this point have no practical significance. A trend of increasing relative error values can be observed after the equilibrium point, possibly due to the low magnitude of the moisture ratio values, which may lead to imprecision in the results beyond that stage.

On the other hand, it is also observed that, within the appropriate drying time range for each temperature, the relative error values remain low, indicating excellent agreement between the two solutions. However, it is important to note that the infinite series solution of the diffusion equation can never yield an exact value for the moisture ratio when truncated to a finite number of terms. Nevertheless, it can approximate the true value with high precision as the number of terms increases. In the present case, a value of $MR(0) \approx 0.98$ was obtained, while the exact theoretical value at $t = 0$ is $M_R(0) = 1$, by definition.

In addition to these observations, it is almost impossible to distinguish differences in the drying curves shown in the graph in Figure 2, indicating that either of the two solutions can be used interchangeably to obtain similar results. The choice between them will depend on the intended use of the results and the type of analysis to be performed. The agreement between the two solutions is further supported by the low values of the standard error of the estimates (SEE).

Table 4 Comparison of the moisture ratio of a cowpea grain (Vigna unguiculata (L.) Walp.), considering ellipsoidal geometry and 30 terms of the series solution of the diffusion equation, with the numerical solution using finite elements, through the Relative Error (***Error***) and the Standard Error of the Estimates (***SEE***).

Temp. (h)	**Water Content Ratio** $M_R(t)$								
	$T_a = 40$°C			$T_a = 60$°C			$T_a = 70$°C		
	Anal. Series	Finite Elem.	Error (%)	Anal. Series	Finite Elem.	Error (%)	Anal. Series	Finite Elem.	Error (%)
0	0.980	0.977	0.36	0.980	0.978	0.19	0.980	0.980	0.00
1	0.685	0.684	0.13	0.517	0.516	0.14	0.422	0.424	0.71
2	0.573	0.576	0.56	0.366	0.373	1.89	0.259	0.258	0.54
3	0.495	0.495	0.09	0.270	0.270	0.18	0.166	0.165	0.34
4	0.433	0.432	0.25	0.202	0.205	1.20	0.107	0.109	1.95
5	0.383	0.380	0.62	0.153	0.154	0.60	0.069	0.069	0.39
6	0.340	0.339	0.52	0.115	0.112	3.27	0.045	0.045	1.58
7	0.304	0.300	1.21	0.087	0.090	3.47	0.029	0.031	5.71
8	0.272	0.273	0.51	0.066	0.072	8.18	0.019	0.018	1.45
9	0.244	0.240	1.40	0.050	0.048	4.36	0.012	0.014	17.13
10	0.219	0.216	1.56	0.038	0.038	0.28	0.008	0.010	32.87
11	0.197	0.194	1.32	0.029	0.029	0.60	0.005	0.006	14.17
12	0.177	0.174	1.74	0.022	0.022	0.81			
13	0.160	0.157	1.88	0.017	0.015	7.07			
14	0.144	0.141	1.97	0.013	0.014	8.66			
15	0.130	0.134	3.55	0.010	0.009	0.45			

16	0.117	0.117	0.02	0.007	0.009	27.56			
17	0.105	0.106	0.57	0.005	0.007	34.03			
18	0.095	0.094	1.08						
19	0.086	0.089	4.15						
20	0.077	0.078	1.57						
	$\boldsymbol{SEE = 0,00150}$			$\boldsymbol{SEE = 0,00154}$			$\boldsymbol{SEE = 0,00148}$		

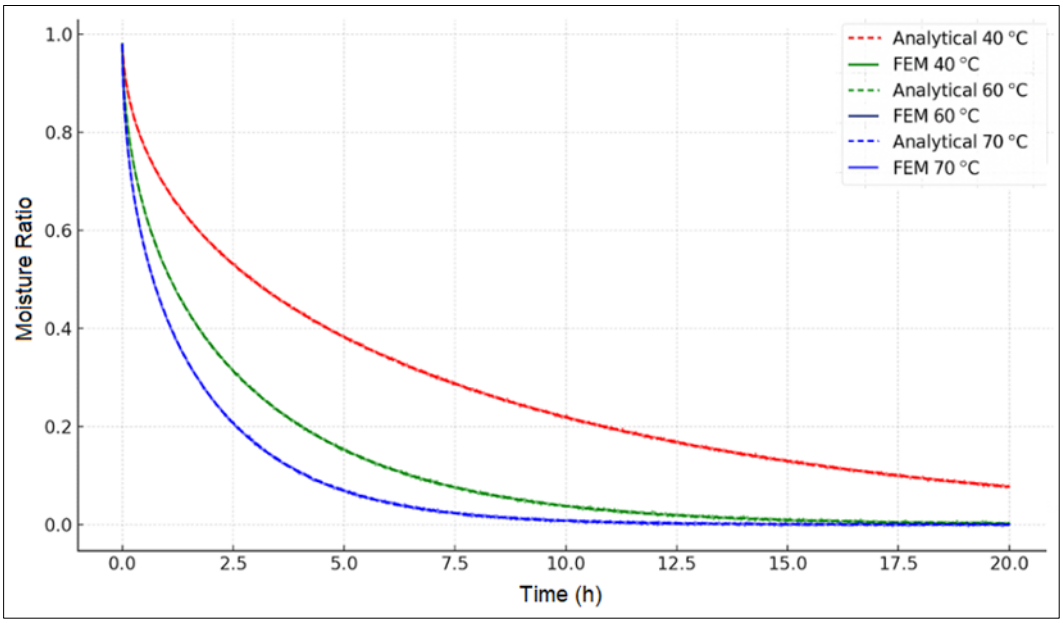

Figure 2 Comparison of the moisture ratio $\boldsymbol{M_R}$ of a cowpea grain, considering ellipsoidal geometry and 30 terms of the series solution of the diffusion equation, with the numerical solution using finite elements.

5. Conclusion

Drying occurs more rapidly at higher temperatures—a behavior consistently observed due to the increase in effective diffusivity with temperature (Li et al., 2023). This enhancement intensifies the driving force of the process, facilitating the transport of moisture from the interior to the surface of the grain along a concentration gradient.

The comparison between the analytical solution of Fick's law using a 30-term series and the numerical solution via the Finite Element Method (FEM) for simulating the drying of a cowpea bean grain—modeled as an ellipsoid and subjected to varying temperatures—demonstrates excellent agreement between the two approaches. Low relative errors were consistently observed throughout the simulations, confirming the reliability of both models.

The drying curves generated by the FEM closely matched those obtained analytically, reinforcing the accuracy of the numerical method. Minor oscillations in the numerical results, inherent to the discretization process, do not compromise the overall validity of the simulation.

A significant advantage of the Finite Element Method lies in its flexibility to handle complex geometries, making it particularly suitable for modeling irregular or anisotropic domains such as agricultural grains.

To support the development of increasingly precise models, experimental studies under controlled conditions are recommended. These studies would provide robust data on the physical properties of cowpea grains, enabling more accurate and tailored simulations for this specific material.

Compliance with ethical standards

Disclosure of conflict of interest

No conflict of interest to be disclosed.

References

[1] Albini, G., Freire, F. B., & Freire, J. T. (2019). Capítulo 4 – Modelagem e simulação da transferência de calor e massa: estudo de caso para secagem de grãos de cevada em leito fixo. In J. T. Freire & G. Albini (Orgs.), Tópicos Especiais em Sistemas Particulados – Volume 5 (pp. 91–116). São Carlos: Editora da UFSCar. ISBN 978-85-913116-3-7.

[2] Arsène, M., Hénault, C., & Lefebvre, J. (2021). CFD modeling of drying kinetics and moisture transport in agricultural grains. Food and Bioproducts Processing, 124, 126-134. https://doi.org/10.1016/j.fbp.2021.04.012

[3] ASAE Standards (2003). Moisture relationships of plant-based agricultural products.

[4] ASHRAE Handbook (2017). Fundamentals. American Society of Heating, Refrigerating and Air-Conditioning Engineers.

[5] Bengtsson, G., & Ahrné, L. (2005). Drying and storage of grains and oilseeds. Springer.

[6] Bird, R. B., Stewart, W. E., & Lightfoot, E. N. (2002). Transport phenomena (2nd ed.). Wiley.

[7] Brooker, D. B., & Bakker-Arkema, F. W. (1974). Drying cereal grains. AVI Publishing Company.

[8] Brooker, D. B., Bakker-Arkema, F. W., & Hall, C. W. (1992). Drying and storage of grains and oilseeds. The AVI Publishing Company.

[9] Chen, C., & Pan, Z. (2023). An overview of progress, challenges, needs and trends in mathematical modeling approaches in food drying. Drying Technology, 41(16), 2586-2605. https://doi.org/10.1080/07373937.2023.2207636

[10] COMSOL Multiphysics Reference Guide (2023). Heat Transfer and Transport of Diluted Species Interfaces.

[11] COMSOL. (2017). COMSOL Multiphysics: A simulation software platform for multiphysics modeling. COMSOL, Inc. Retrieved from https://www.comsol.com/comsol-multiphysics

[12] Corrêa, P. C., et al. (2007). Drying and storage of agricultural products. UFV Publisher.

[13] Crank, J. (1975). The Mathematics of Diffusion. 2nd ed. Oxford University Press.

[14] Dincer, I., & Dost, S. (2019). A review of modeling techniques for grain drying processes. Journal of Food Engineering, 242, 42-53. https://doi.org/10.1016/j.jfoodeng.2018.10.003

[15] Erdogdu, F. (2023). Mathematical modeling of food thermal processing: Current and future challenges. Current Opinion in Food Science, 51, 101042. https://doi.org/10.1016/j.cofs.2023.101042

[16] Fick, A. (1855). Ueber diffusion. Annalen der Physik, 170(1), 59–86.

[17] Fish, J., & Belytschko, T. (2007). A first course in finite elements. John Wiley & Sons.

[18] Freire Filho, F. R., Ribeiro, V. Q., Rocha, M. de M., Damasceno e Silva, K. J., Nogueira, M. do S. da R., & Rodrigues, E. V. (2012). Production, breeding and potential of cowpea crop in Brazil. Embrapa Mid-North. Retrieved from https://www.researchgate.net/publication/273138062_Production_breeding_and_potential_of_cowpea_crop_in_Brazil

[19] Goneli, A. L. D., Corrêa, P. C., Oliveira, G. H. H., & Botelho, F. M. (2010). Water desorption and thermodynamic properties of common bean grains. Journal of Food Process Engineering, 33(5), 826–843. https://doi.org/10.1111/j.1745-4530.2008.00299.x:contentReference[oaicite:1]{index=1}

[20] Haghighi, K., Irudayaraj, J., Stroshine, R. L., & Sokhansanj, S. (1990). Grain kernel drying simulation using the finite element method. Transactions of the ASAE, 33(6), 1957–1965. https://doi.org/10.13031/2013.31564

[21] Harris, C. R., Millman, K. J., van der Walt, S. J., Gommers, R., Virtanen, P., Cournapeau, D., ... & Oliphant, T. E. (2020). Array programming with NumPy. Nature, 585(7825), 357–362. https://doi.org/10.1038/s41586-020-2649-2

[22] Henderson, S. M., & Pabis, S. (1961). Grain drying theory. Part I: Temperature effects on drying coefficients. Journal of Agricultural Engineering Research, 6(3), 169-174. https://doi.org/10.1016/S0021-8634(61)80047-1

[23] Ho, Q. (1992). Microwave drying of food: Principles, methods, and applications. Springer.

[24] Hunter, J. D. (2007). Matplotlib: A 2D graphics environment. Computing in Science & Engineering, 9(3), 90–95. https://doi.org/10.1109/MCSE.2007.55

[25] Incropera, F. P., DeWitt, D. P., Bergman, T. L., & Lavine, A. S. (2007). Fundamentals of Heat and Mass Transfer. 6th edition. John Wiley & Sons.

[26] Iqbal, M., Haider, Z., & Sattar, A. (2020). CFD-based modeling for grain drying with heterogeneous moisture distribution. Drying Technology, 38(8), 1061-1075. https://doi.org/10.1080/07373937.2019.1663293

[27] Irudayaraj, J. M. K. (1993). Finite element simulation of viscoelastic biomaterial behavior during drying (Doctoral dissertation, Purdue University).

[28] Jamaleddine, T., & Ray, M. (2010). Application of computational fluid dynamics for simulation of drying processes: A review. Drying Technology, 28(1), 120-154. https://doi.org/10.1080/07373930903517458

[29] Jayas, D. S., Alagusundaram, K., & White, N. G. (2023). Drying of grains: A review. Drying Technology, 11(7), 1658-1682.

[30] Jia, C.-C., Yang, W., Siebenmorgen, T. J., & Cnossen, A. G. (2002). Development of computer simulation software for single grain kernel drying, tempering, and stress analysis. Transactions of the ASAE, 45(5), 1485–1492. https://doi.org/10.13031/2013.11039

[31] Jian, F., & Jayas, D. S. (2022). Grains: Engineering fundamentals of drying and storage. CRC Press.

[32] Jibril, A.N., Zhang, X., Wang, S., Bello, ZA, Henry, II, & Chen, K. (2024). Far-infrared drying influence on machine learning algorithms in improving corn drying process with graphene irradiation heating plates. Journal of Food Process Engineering, 47(4), e14603. https://doi.org/10.1111/jfpe.14603

[33] Jimoh, K. A., Hashim, N., Shamsudin, R., Che Man, H., Jahari, M., & Onwude, D. I. (2023). Recent advances in the drying process of grains (Jimoh et al., 2023). Food Engineering Reviews, 15, 548–576.

[34] Kaveh, M., Najafpour, G., & Mohammadi, M. (2022). Effects of ultrasound pre-treatment combined with microwave drying on kiwifruit slices: Optimization of drying time, energy consumption, and product quality using response surface methodology. Journal of Food Processing and Preservation, 46(5), e16714. https://doi.org/10.1111/jfpp.16714

[35] Lewis, W. K. (1921). The rate of drying of solid materials. Journal of Industrial & Engineering Chemistry, 13(5), 427-432.

[36] Li, X., Wang, Y., Yang, K., & Du, X. (2023). Numerical study of heat and mass transfer during drying process of barley grain piles based on the pore scale. Journal of Food Process Engineering, 46(11), e14433.

[37] Liu, W., Chen, G., Zheng, D., Ge, M., & Liu, C. (2023). Numerical and experimental investigation of flow and heat transfer in a fixed bed of non-spherical grains using the DEM-CFD method. Journal of Food Process Engineering, 46(8), e14362. https://doi.org/10.1111/jfpe.14362

[38] Liu, Z., Zhang, Y., & Wang, Q. (2017). Application of CFD in drying technology: Simulation and experimental validation for grains. Drying Technology, 35(11), 1376-1385. https://doi.org/10.1080/07373937.2017.1336516

[39] Madamba, P. S. (1996). Thin-layer drying models for agricultural products: a review. Drying Technology, 14(10), 1977–2004.

[40] Oliveira, G. H. H, et al. (2014). Mathematical modeling of drying of beans (Phaseolus vulgaris L.) in thin layer. Brazilian Journal of Agricultural and Environmental Engineering, 18(10), 1051–1057.

[41] Pabis, S., Jayas, D. S., & Cenkowski, S. (1991). Grain drying: Theory and practice. Wiley.

[42] Page, G. E. (1949). Factors Influencing the Maximum Rates of Air Drying Shelled Corn in Thin Layers. MS Thesis, Purdue University, West Lafayette, IN.

[43] Patankar, S. V. (1980). Numerical heat transfer and fluid flow. Taylor & Francis.

[44] Pham, Q. T. (1986). Modeling of heat and mass transfer (Bird et al., 2002) in food processing. International Journal of Refrigeration, 9(6), 365–373.

[45] Ramachandran, R. P., Akbarzadeh, M., Paliwal, J., & Cenkowski, S. (2018). Computational fluid dynamics in drying process modeling—a technical review. Food Bioprocess Technology, 11, 271–292.

[46] Resende, O., Corrêa, PC, et al. (2005). Experimental determination of effective diffusivity (Li et al., 2023) and activation energy in grain drying. Agricultural Engineering, 13(4), 252–263.

[47] Resende, O., et al. (2008). Mathematical modeling of the drying process of beans (Phaseolus vulgaris L.). Science and Agrotechnology, 32(3), 883–889.

[48] Sahin, S., & Sumnu, G. (2006). Food dehydration: Theory and practice. Springer.

[49] Tian, X., Wang, W., & Chen, X. (2016). Numerical study on moisture distribution and drying behavior of agricultural products using CFD. Computers and Electronics in Agriculture, 126, 126-135. https://doi.org/10.1016/j.compag.2016.06.015

[50] Virtanen, P., Gommers, R., Oliphant, T. E., Haberland, M., Reddy, T., Cournapeau, D., ... & van Mulbregt, P. (2020). SciPy 1.0: Fundamental algorithms for scientific computing in Python. Nature Methods, 17(3), 261–272. https://doi.org/10.1038/s41592-019-0686-2

[51] Weller, H. G., Tabor, G., Jasak, H., & Fureby, C. (1998). A new approach to computational fluid dynamics: The OpenFOAM toolbox. Computers in Physics, 12(6), 618-629. https://doi.org/10.1063/1.168744

[52] Zhang, M., Wang, S., & Mujumdar, A. S. (2006). Drying of agricultural products. Science Press.

[53] Zhang, Y., Liu, Z., & Wang, Q. (2019). CFD modeling of the drying process for agricultural grains. Journal of Food Engineering, 234, 57-64. https://doi.org/10.1016/j.jfoodeng.2018.09.011